

NASA/TM-2009-215955



# Experimental Behavior of Fatigued Single Stiffener PRSEUS Specimens

*Dawn C. Jegley  
Langley Research Center, Hampton, Virginia*

---

December 2009

## NASA STI Program . . . in Profile

Since its founding, NASA has been dedicated to the advancement of aeronautics and space science. The NASA scientific and technical information (STI) program plays a key part in helping NASA maintain this important role.

The NASA STI program operates under the auspices of the Agency Chief Information Officer. It collects, organizes, provides for archiving, and disseminates NASA's STI. The NASA STI program provides access to the NASA Aeronautics and Space Database and its public interface, the NASA Technical Report Server, thus providing one of the largest collections of aeronautical and space science STI in the world. Results are published in both non-NASA channels and by NASA in the NASA STI Report Series, which includes the following report types:

- **TECHNICAL PUBLICATION.** Reports of completed research or a major significant phase of research that present the results of NASA programs and include extensive data or theoretical analysis. Includes compilations of significant scientific and technical data and information deemed to be of continuing reference value. NASA counterpart of peer-reviewed formal professional papers, but having less stringent limitations on manuscript length and extent of graphic presentations.
- **TECHNICAL MEMORANDUM.** Scientific and technical findings that are preliminary or of specialized interest, e.g., quick release reports, working papers, and bibliographies that contain minimal annotation. Does not contain extensive analysis.
- **CONTRACTOR REPORT.** Scientific and technical findings by NASA-sponsored contractors and grantees.
- **CONFERENCE PUBLICATION.** Collected papers from scientific and technical conferences, symposia, seminars, or other meetings sponsored or co-sponsored by NASA.
- **SPECIAL PUBLICATION.** Scientific, technical, or historical information from NASA programs, projects, and missions, often concerned with subjects having substantial public interest.
- **TECHNICAL TRANSLATION.** English-language translations of foreign scientific and technical material pertinent to NASA's mission.

Specialized services also include creating custom thesauri, building customized databases, and organizing and publishing research results.

For more information about the NASA STI program, see the following:

- Access the NASA STI program home page at <http://www.sti.nasa.gov>
- E-mail your question via the Internet to [help@sti.nasa.gov](mailto:help@sti.nasa.gov)
- Fax your question to the NASA STI Help Desk at 443-757-5803
- Phone the NASA STI Help Desk at 443-757-5802
- Write to:  
NASA STI Help Desk  
NASA Center for AeroSpace Information  
7115 Standard Drive  
Hanover, MD 21076-1320

NASA/TM-2009-215955



# Experimental Behavior of Fatigued Single Stiffener PRSEUS Specimens

*Dawn C. Jegley*  
*Langley Research Center, Hampton, Virginia*

National Aeronautics and  
Space Administration

Langley Research Center  
Hampton, Virginia 23681-2199

---

December 2009

The use of trademarks or names of manufacturers in this report is for accurate reporting and does not constitute an official endorsement, either expressed or implied, of such products or manufacturers by the National Aeronautics and Space Administration.

Available from:

NASA Center for AeroSpace Information  
7115 Standard Drive  
Hanover, MD 21076-1320  
443-757-5802

## Abstract

*NASA, the Air Force Research Laboratory and The Boeing Company have worked to develop new low-cost, light-weight composite structures for aircraft. A Pultruded Rod Stitched Efficient Unitized Structure (PRSEUS) concept has been developed which offers advantages over traditional metallic structure. In this concept a stitched carbon-epoxy material system has been developed with the potential for reducing the weight and cost of transport aircraft structure by eliminating fasteners, thereby reducing part count and labor. By adding unidirectional carbon rods to the top of stiffeners, the panel becomes more structurally efficient. This combination produces a more damage tolerant design. This document describes the results of experimentation on PRSEUS specimens loaded in unidirectional compression in fatigue and to failure.*

## Introduction

NASA, the Air Force Research Laboratory and The Boeing Company have worked to develop new low-cost, light-weight composite structures for aircraft. A Pultruded Rod Stitched Efficient Unitized Structure (PRSEUS) concept has been developed which offers advantages over traditional metallic structure (ref 1-4). In this concept a stitched carbon-epoxy material system has been developed with the potential for reducing the weight and cost of commercial transport aircraft structure. By stitching through the thickness of a dry carbon-epoxy material system, the labor associated with panel fabrication and assembly can be significantly reduced. When stitching through the thickness of pre-stacked skin, stringers, intercostals and spar caps, the need for mechanical fasteners is almost eliminated. This manufacturing approach reduces part count, and therefore, cost of the structure. In addition, stitching reduces delamination and improves damage tolerance, allowing for a lighter structure with more gradual failures than traditional composites without through-the-thickness reinforcement. However, the PRSEUS concept is relatively new and the behavior of PRSEUS specimens must be evaluated to understand both fatigue and failure response.

The PRSEUS concept consists of carbon-epoxy panels fabricated from dry components and then infused using high temperature and vacuum pressure only. No autoclave is required. Skins, flanges and webs are composed of layers of graphite material forms that are prekitted in multi-ply stacks using Hercules, Inc. AS4 fibers. Several stacks of the prekitted material are used to build up the desired thickness and configuration. Specimens are stitched together using Vectran fibers. Stiffener flanges were stitched to the skin and no mechanical fasteners are used for joining. To maintain the panel geometry during fabrication, first stiffeners and then the skin are placed in a stitching tool for assembly prior to moving to a curing tool for consolidation in the oven. The stiffeners running in the axial direction consist of webs with a bulb of unidirectional carbon fiber rods at the top of the web. AS4 carbon fiber overwraps surround the bulb. The stiffeners in the lateral direction are foam filled hats.

In the current study each pre-kitted stack had a  $[45/-45/0_2/90/0_2/-45/45]_T$  laminate stacking sequence. Stack thickness was approximately 0.052 inches. For this study specimens were cut from a large PRSEUS panel that had seven rod-stiffeners with 6-inch spacing and three frames with 20-inch spacing. This panel was fabricated under a NASA contract to The Boeing Company entitled “Damage Arresting Composites for Shaped Vehicles.” A photograph of this panel is shown in figure 1. All specimens were made from AS4 fibers and HexFlow VRM 34 resin, as described in ref. 1. The rods were Toray unidirectional T800 fiber with a 3900-2B resin and frame stiffeners were filled with Rohacell foam. A sketch of the intersection of rod and frame elements is shown in figure 2.



Figure 1. Cured panel prior to extraction of test specimens.

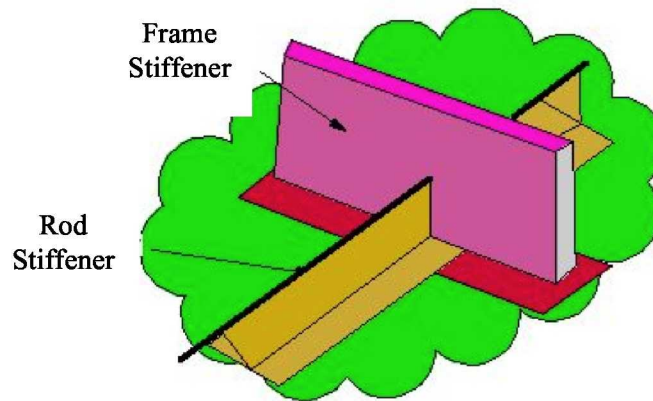
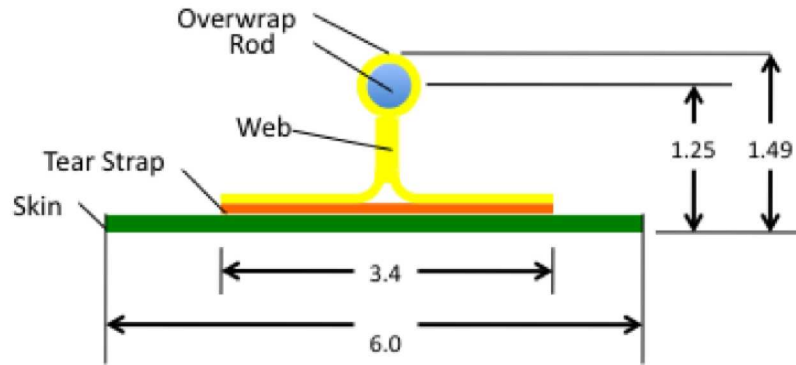


Figure 2. PRSEUS stiffener intersection.

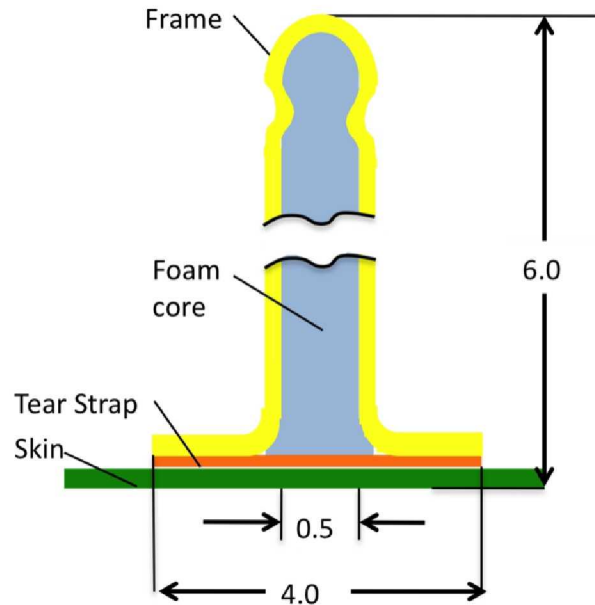
## Test Specimen Description

Two specimens with a single axial stiffener, herein identified as rod-stiffened specimens R3 and R4, and two specimens with a central hat-stiffener representative of a fuselage frame, herein identified as frame specimens F3 and F4, were examined in this study. Sketches of the cross section of each type of specimen are shown in figure 3 and photographs of each specimen are shown in figure 4. Nominal skin

thickness was 0.052 inches. Rod-stiffeners had a 3.4-inch wide flange, a 0.104 inch-thick stiffener web and a 1.5-inch tall stiffener. Flange thickness was half the blade or web thickness. One stack of additional material was added under each flange as tear straps or stiffener caps. These reinforcing layers covered the same area of skin as the stiffener flange. Frame stiffeners had a 4.0-inch wide flange and a 6.0-inch tall stiffener. Rod-stiffened specimens were 18 inches tall and 6 inches wide while frame specimens were 16.6 inches tall and 10 inches wide. Prior to testing, each end of the specimen was potted in 1.0-inch-deep epoxy compound and the ends were ground flat and parallel to each other to ensure uniform load introduction. Rod-stiffened specimens contained no frames while frame specimens contained one frame in the loading direction and two rod-stiffeners which were six inches apart, perpendicular to the frames.

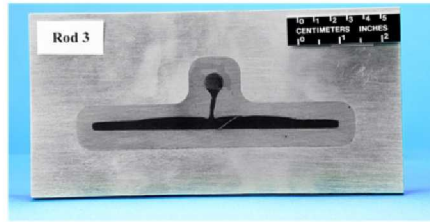


a) Rod stiffener.

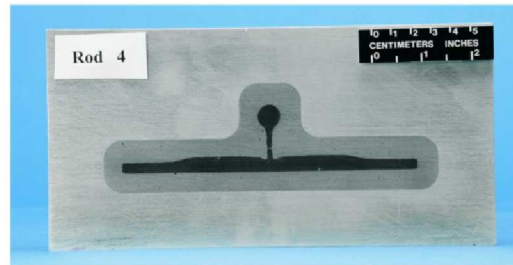


b) Frame stiffener.

Figure 3. Stiffener geometry. Dimensions are in inches.



a) Rod specimen R3



b) Rod specimen R4



c) Frame specimen F3

Figure 4. Test specimens.



d) Frame specimen F4

Figure 4. Test specimens-continued.

Detailed measurements of skin and stiffener thicknesses are shown in figure 5. Skin thickness of specimen R3 range from .052 to .061 inches. Skin thickness of specimen R4 range from .049 to .060 inches. Skin thickness of specimen F3 range from .044 to .056 inches. Skin thickness of specimen F4 range from .047 to .060 inches. Rod region diameter averaged .485 inches and frame width averaged .665 inches. Prior to attaching strain gages, the unstiffened surface, herein referred to as the Outer Mold Line (OML), each specimen was scanned using a Coordinate Measurement Machine to document the geometry of the unstiffened surface. The result of these scans is shown in figure 6. Surface measurements were found to range from 0.015 to -.025 inches in the rod specimens and -.008 to .005 inches in the frame specimens. These imperfections correspond to approximately 25% of the skin thickness for the rod specimens and 10% of the skin thickness for the frame specimens.

	Left edge skin	Right edge skin	Stiffener
R3	0.0569	0.0607	0.4891
	0.0519	0.04845	0.4825
	0.0565	0.05735	0.4882
R3 average	0.0551	0.0555	0.4866
R4	0.05670	0.05600	0.48445
	0.04905	0.05370	0.48930
	0.05790	0.05925	0.47915
R4 average	0.05455	0.05631	0.48430
F3	0.05615	0.04755	0.66365
	0.05430	0.04450	0.6660
	0.05645	0.04635	0.6618
F3 average	0.05563	0.04613	0.66381
F4	0.05410	0.04705	0.66285
	0.05475	0.0552	0.66315
	0.06015	0.0514	0.67210
F4 average	0.05633	0.05121	0.66603

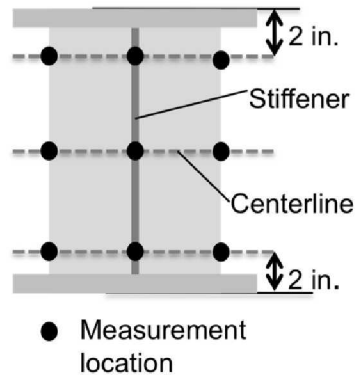


Figure 5. Measured thicknesses. Dimensions are in inches.

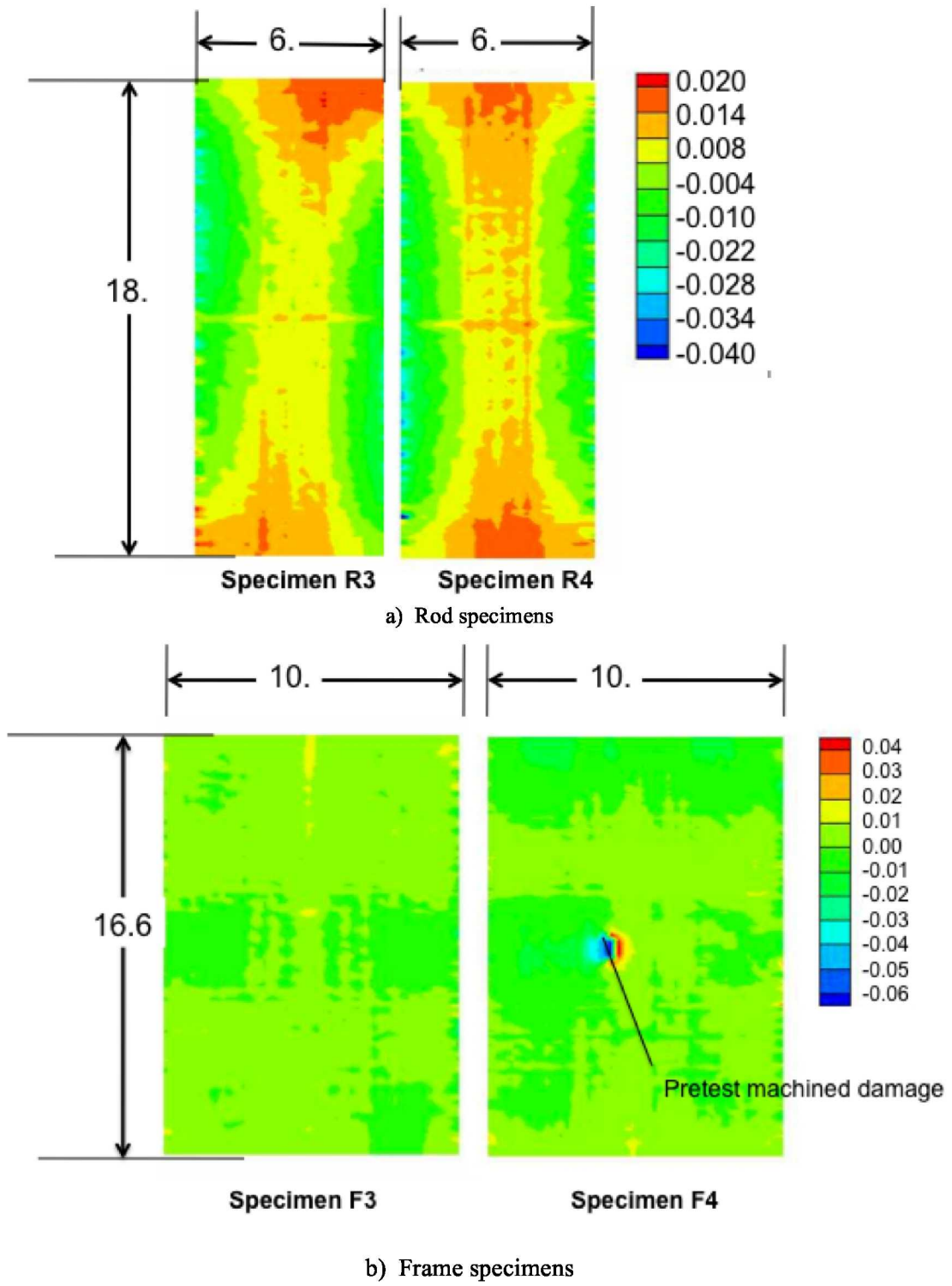


Figure 6. Measured out-of-plane imperfections prior to testing. Dimensions are in inches.

Prior to delivery to NASA the OML of specimen F4 was damaged during the machining process. A photograph of this damage is shown in figure 7. The dent is approximately circular with a 1-inch diameter and the maximum depth is approximately 0.1 inches. No damage at this location is visible on the stiffened or Inner Mold Line (IML) side of the specimen.



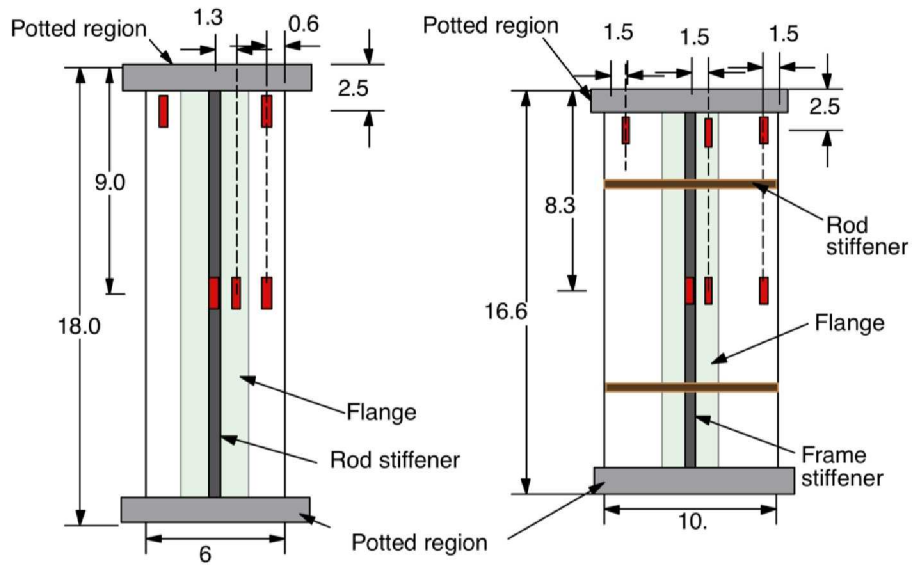
Figure 7. Machining damage to specimen F4.

## Test Procedure and Instrumentation

All specimens were loaded in axial compression. The applied spectrum of 55,000 cycles used for the applied fatigue load. The 55,000 cycles was broken into 11 blocks of 5000 cycles with the maximum loads and load rates shown in table 1 for each cycle. Specimens were loaded in compression only and load was not removed between cycles. After the completion of the fatigue loading, each specimen was loaded to failure in axial compression. Fatigue loading was typically applied at the rate of 1 cycle per second while failure loading was applied at the rate of 5,000 to 10,000 lb/min. Selected intermediate fatigue cycles were performed at a rate of 4,000 to 10,000 lb/min.

Displacement and strain gage data were recorded at the rate of once every second as load was applied during the initial cycle, selected fatigue cycles and during the failure (post-fatigue) test as shown in table 2. Displacements were measured using three displacement transducers measuring end-shortening, and one measuring stiffener motion. An additional transducer measuring out-of-plane motion of the skin at the midlength location was included for the frame specimens. Nine strain gages were added to each rod specimen and ten strain gages were added to each frame specimen in the pattern shown in figures 8. The additional gage on the frame specimens was located on the frame web. Back-to-back strain gages were used to monitor strains in the skin, flanges and stiffeners of each specimen. Metal supports were added to the unloaded edges to restrain out-of-plane motion of the skin while allowing the specimen to deform in-plane. These edge supports for the rod specimens supported IML and OML the full length of the unloaded edge while the lateral rod-stiffeners prevented the edge supports from being continuous along the full length of the frame specimen on the IML. Specimens in the test machine are shown in figure 9. Buckling and failure behavior were noted for each specimen.

An optical measurement system was used to obtain full field displacement and strain results for the OML of each specimen during the post-fatigue test. A photograph showing the Vision Image Correlation (VIC)<sup>4</sup> system is shown in figure 10. A black and white speckle pattern painted on the specimen surface allows the VIC system to track surface motion. Two cameras positioned at different angles to the specimen surface simultaneously photograph the specimen at set intervals during to test. In this case, the specimen was photographed every 5 seconds, resulting in approximately 150 time steps of data. The VIC



Rod specimen
Frame specimen  
 Figure 8. Strain gage patterns. All dimensions are in inches.



Figure 9. Specimens in test machine.

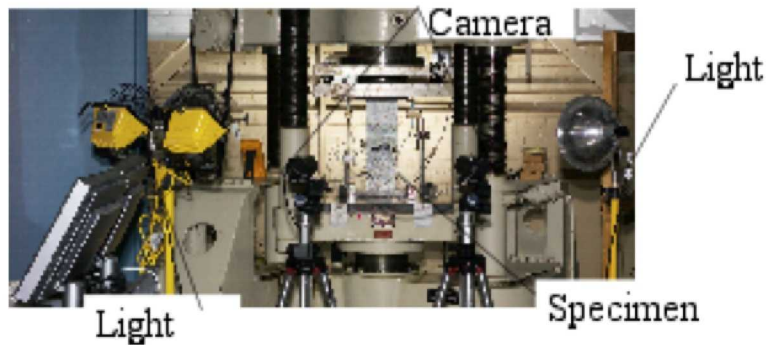


Figure 10. Vision Image Correlation system.

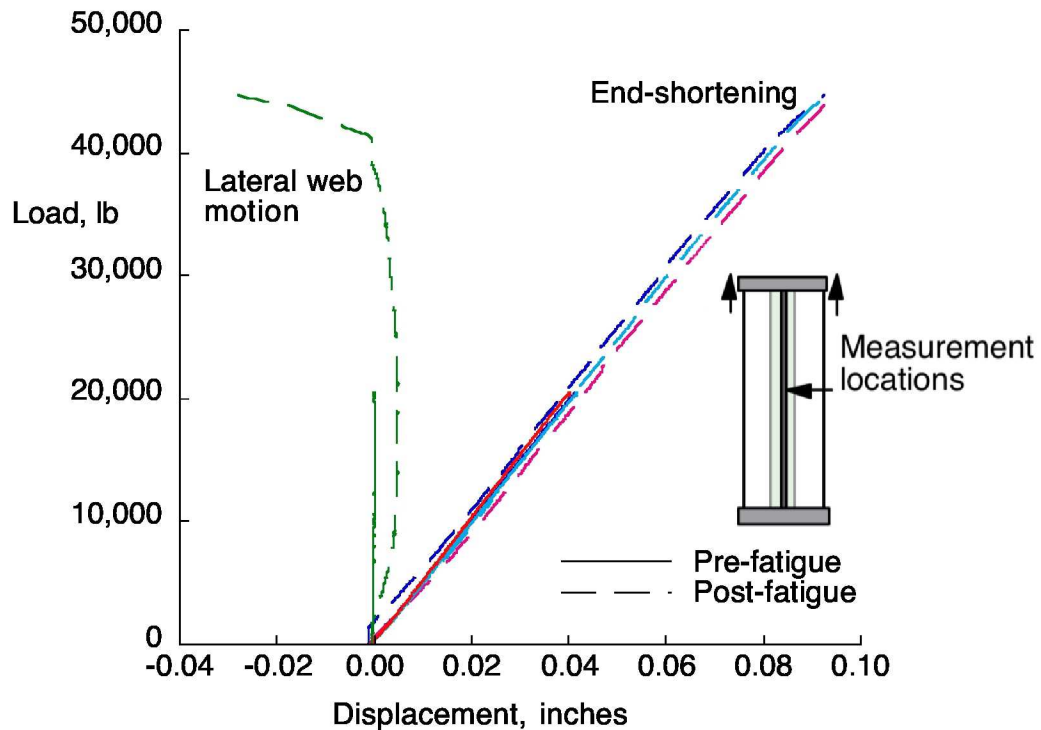
system also records the load from the test machine so images can be related to the corresponding load. The VIC system compares the photographic images and produces three-dimensional displacements and strains at each time step. Since the full-field results are dependent upon the cameras having an unobstructed view of the surface, some local areas where strain gages or wires are removed from the plot or identified as not representing surface behavior in some figures.

## Results and Discussion

Displacements, strains and failure modes are presented herein, followed by a comparison with data obtained previously for specimens subjected only to static loading. Full field results show displacement and strain distributions as the specimen approached failure.

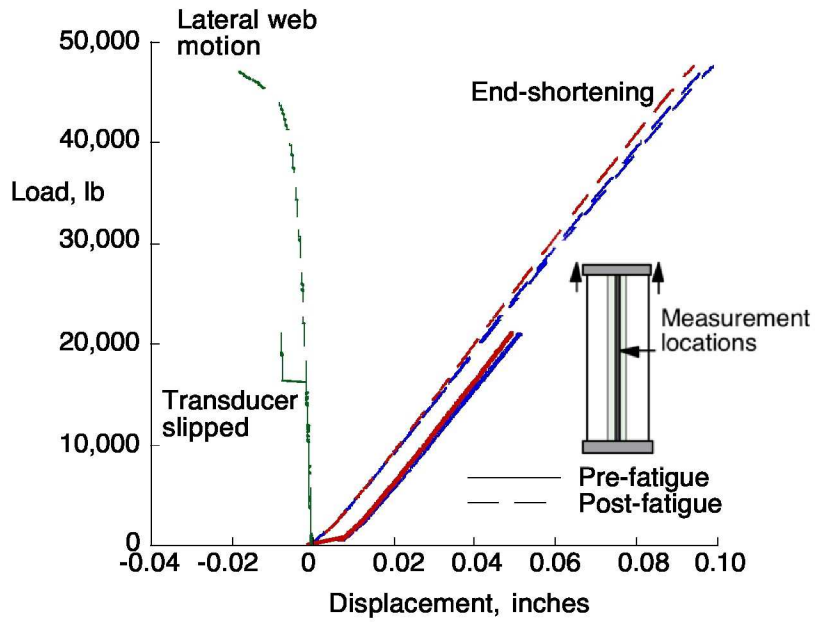
### Displacements and Loads

A comparison of measured displacement as a function of load for end-shortening and out-of-plane deformation from the pre-fatigue loading to 20,500 lb and the post-fatigue loading to failure of rod specimens R3 and R4 is shown in figures 11a and 11b, respectively. Measured displacements for the pre-fatigue loading to 41,000 lb and the post-fatigue loading to failure of frame specimens F3 and F4 is shown in figures 12a and 12b, respectively. Data for the pre-fatigue loading are shown as solid lines and data for the post-fatigue loading are shown as dashed lines. These results indicate that there is no noticeable change in behavior due to the fatigue cycling.



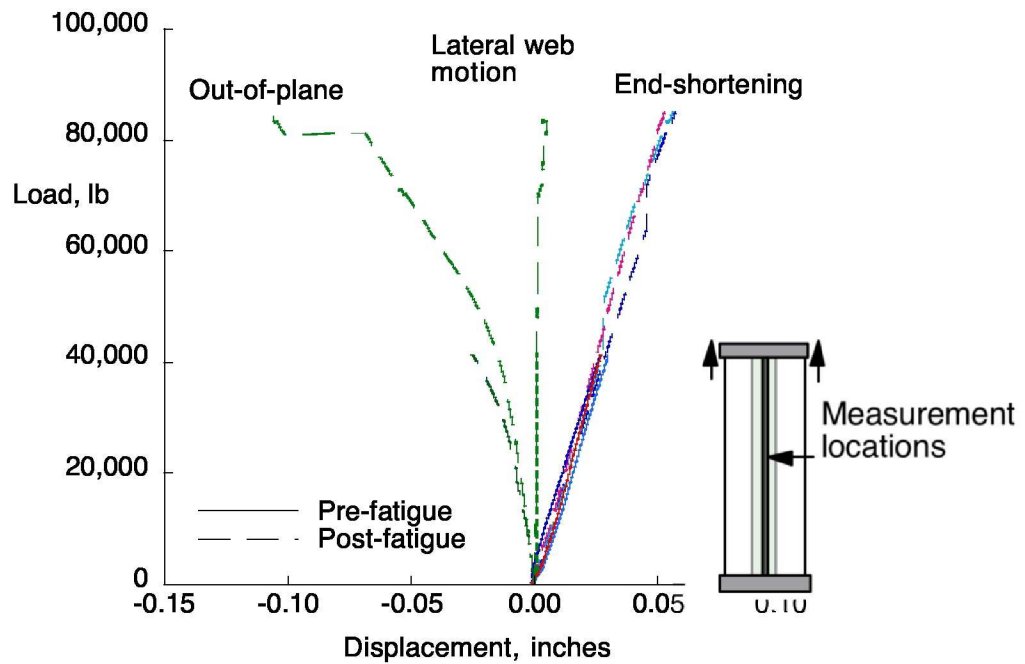
a) Specimen R3

Figure 11. Pre-fatigue and post-fatigue displacements for rod specimens.



b) Specimen R4

Figure 11. Pre-fatigue and post-fatigue displacements for rod specimens-continued.



a) Specimen F3

Figure 12. Pre-fatigue and post-fatigue displacements for frame specimens.

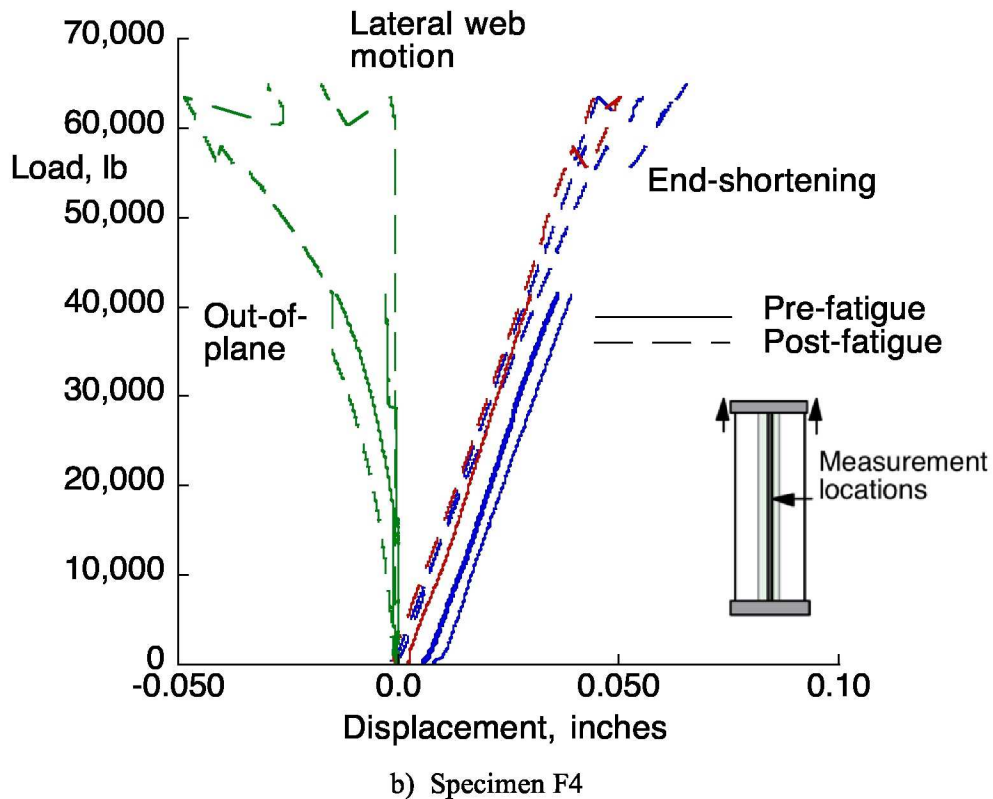


Figure 12. Pre-fatigue and post-fatigue displacements for frame specimens-continued.

Rod specimens failed at loads of approximately 45,000 and 47,654 lb. Frame specimens failed at loads of 85,152 and 64,999 kips. Measured displacements are shown in figures 13 and 14 for the post-fatigue tests of rod and frame specimens, respectively. Data for specimens R3 and F3 are shown as solid lines and data for specimens R4 and F4 are shown as dashed lines. End-shortening results indicate a uniform displacement was applied to the end of specimens R3 and R4. For example, end-shortening results among the three transducers differ by no more than 2% for a load of 4,000 lb and a load of 5% for a load of 40,000 lb for specimen R4. Similar uniform shortening results are seen for specimen F3 however some discontinuities in the slope of the end-shortening results for specimens F3 and F4 indicate some slippage in the transducers or in the platen for loads greater than 40,000 lb. This discontinuity could not be reproduced for a dummy specimen using the same test arrangement.

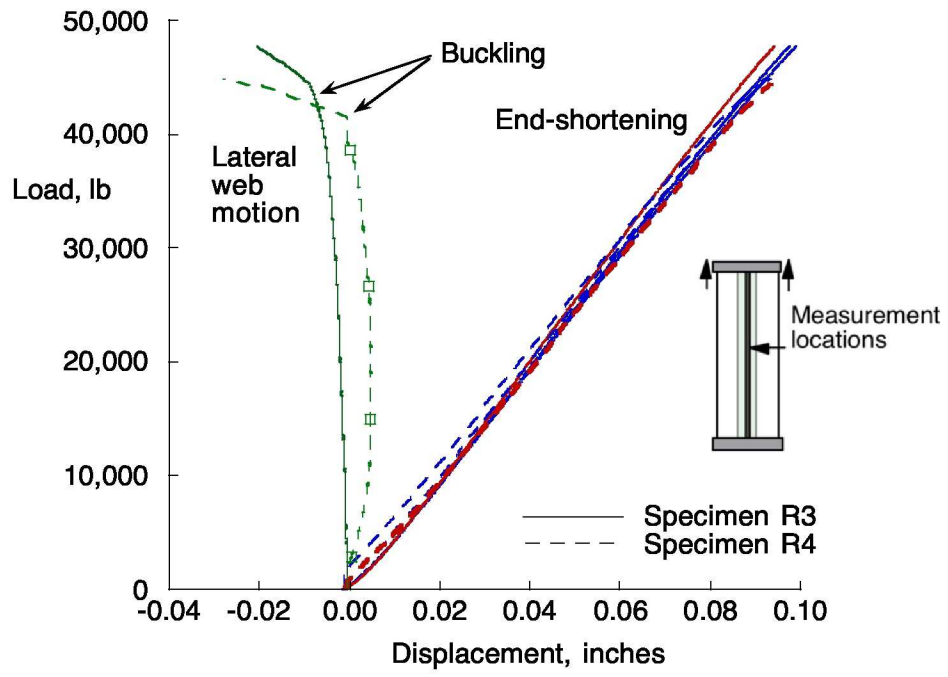


Figure 13. Post-fatigue displacements for rod specimens.

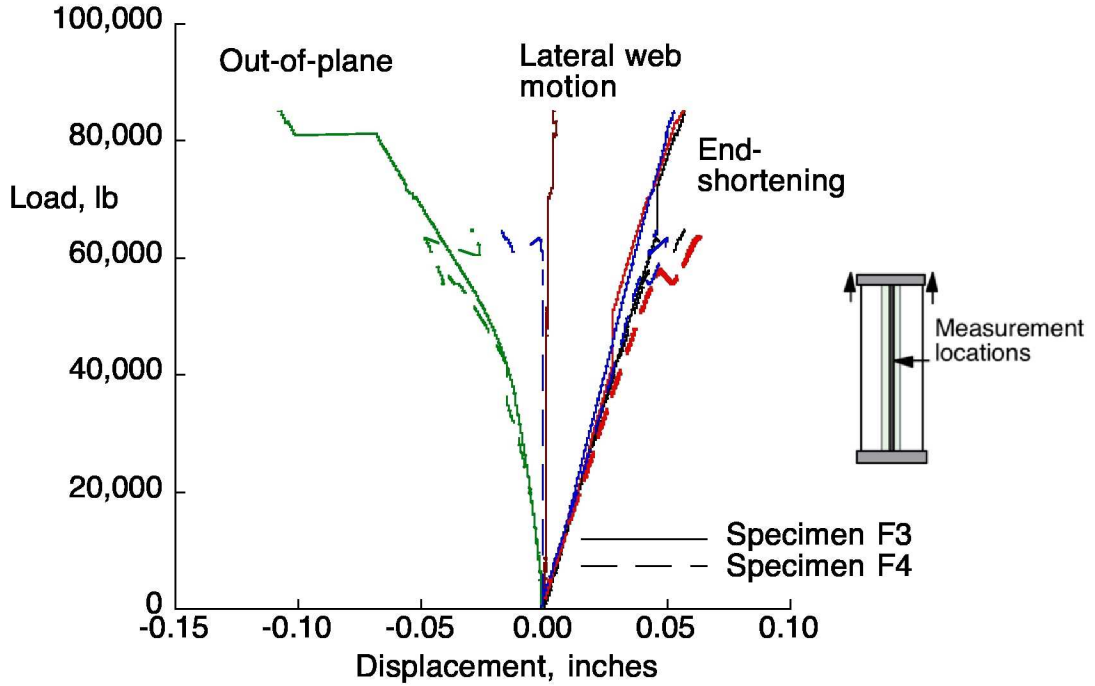


Figure 14. Post-fatigue displacements for frame specimens.

The transducer on the stiffener indicates rolling of the web of the rod specimen at approximately 42,000 lb. The frame of specimens F3 and F4 did not roll. The out-of-plane displacement measurement at the axial centerline of the frame specimens indicates that the edge supports did not fully restrain out-of-plane motion at the unloaded edges. These restraints consisted of individual aluminum pieces held at the top and bottom of the specimen but they were not continuous on the stiffened side because the rod stiffeners went to the edge of the specimen (see figure 4). In addition, these restraints were held in place by screws and the vibration of the system during cycling caused the screws to back out. The screws were tightened after every 2-3 blocks and no damage was evident based on this flexibility.

Full-field results for out-of-plane deformation at approximately the maximum applied load are shown in figure 15 and 16 for rod and frame specimens, respectively. These results indicate rod specimens buckled prior to failure but frame specimens did not. In the rod specimens the centerline where the rod stiffener was located did not move out-of-plane during loading while the unloaded edges did move out of plane despite the edge restraints. A buckle pattern of approximately three half waves developed in each rod specimen. In each rod specimen one edge moved forward in the positive z direction while the other edge moved in the negative z direction about the same magnitude. In the full-field results, regions where strain gages and wires obscure the specimen surface are removed from the plot. In the undamaged frame specimen the out-of-plane displacements were localized to the corners and midlength location. Bending between the lateral support of the potting and rods is evident. The midlength location is half way between rod stiffeners. The primary deformation seen in the damaged frame specimen is in the region of the damage. The displacements shown are the difference between the surface prior to loading and just before failure.

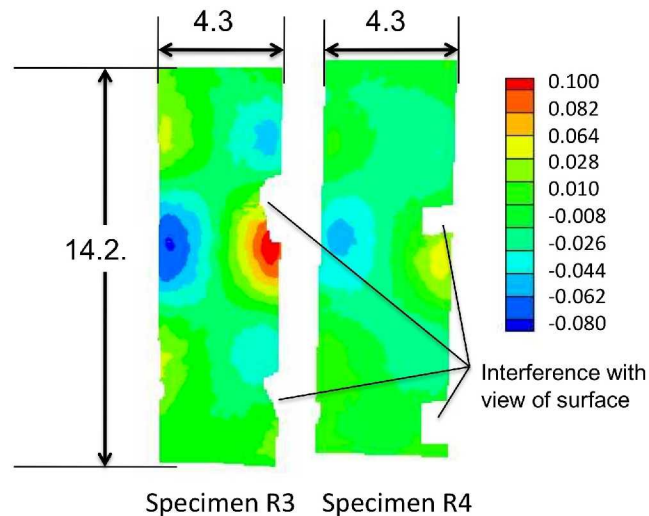
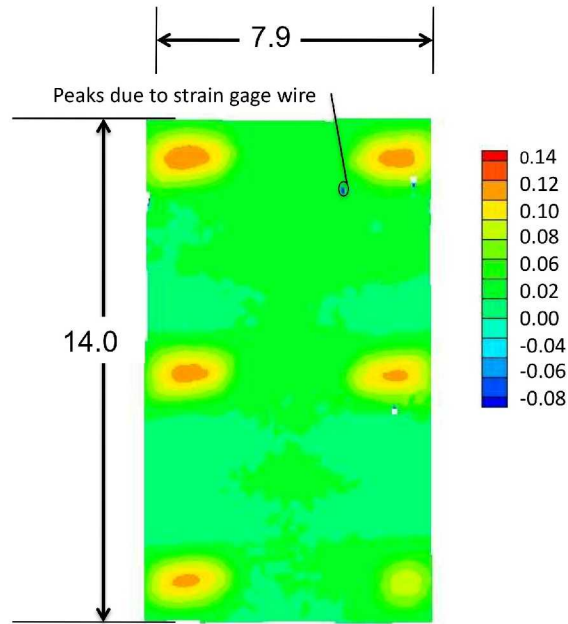
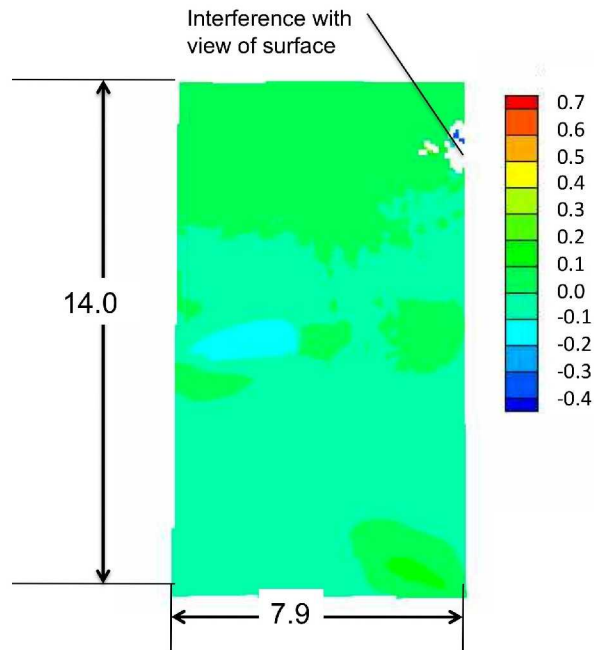


Figure 15. Full-field out-of-plane displacement for rod-stiffened specimens immediately prior to failure. Dimensions are in inches.



a) Frame specimen F3 immediately prior to failure



b) Frame specimen F4 immediately prior to failure

Figure 16. Full-field out-of-plane displacement change from pre-fatigue condition for frame specimens. Dimensions are in inches

## Strain

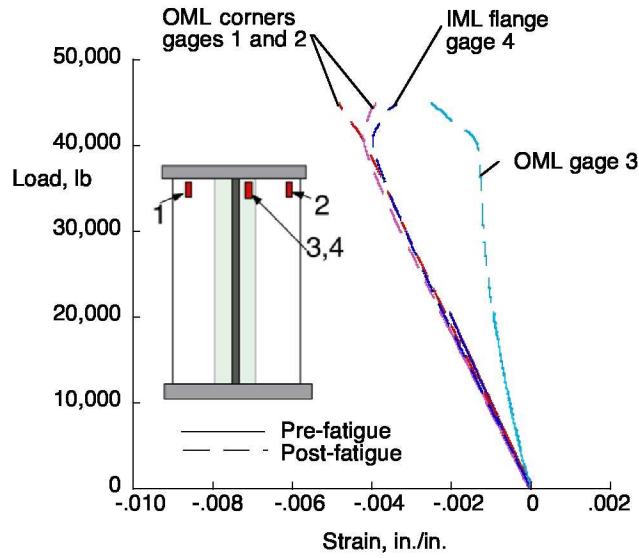
The load-strain relationship for skin and stiffener locations for the first cycle in the fatigue spectrum and the post-fatigue failure test are shown in figures 17 and 18 for rod and frame specimens, respectively. Strain gage locations are shown in the figures. Data for the pre-fatigue loading are shown as solid lines and data for the post-fatigue loading are shown as dashed lines with. A comparison of the skin, flange and rod strains before and after fatigue cycling indicates that the fatigue cycling had no noticeable effect on the strain behavior of specimens R3 and R4. A comparison of the skin, flange and frame strains before and after fatigue cycling indicates that the fatigue cycling had no noticeable effect on the strain behavior of specimens F3 and F4, despite the visible damage in specimen F4 prior to loading.

The load-strain relationship for post-fatigue failure tests of rod and frame specimens are shown in figures 19 and 20, respectively. Strain gage locations are shown in the figure and the green dot in the center of the sketch indicates the location of the pre-test damage in specimen F4. The Strains indicate nonlinear behavior initiates in the OML gages (1 and 2) at approximately 23,000 lb for specimen R4 and 38,000 lb for specimen R3. Buckling is not indicated prior to approximately 38,000 lb in either specimen. Buckling is indicated at approximately 38,000 lb for R3 and 42,000 lb for R4. Even though flange/skin gages 6 and 7 are back-to-back, they diverge at load initiation. Gages 8 and 9 show no divergence and little nonlinear behavior in either rod specimen until failure.

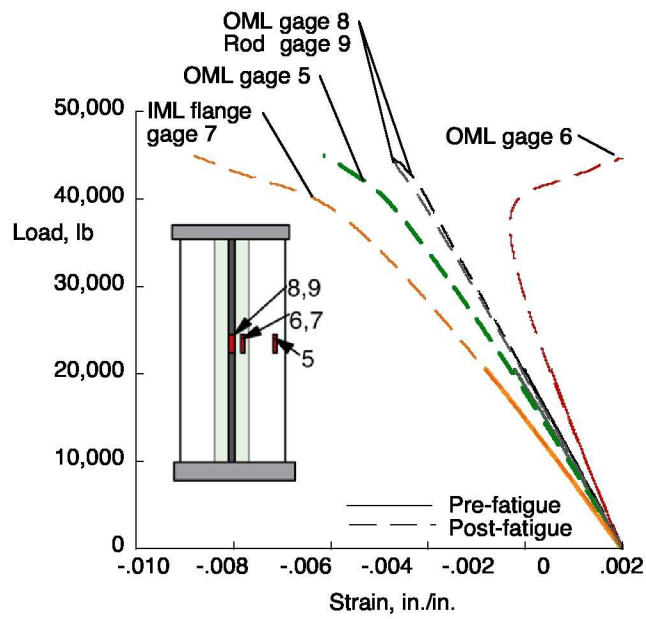
Results for gages away from the pre-test damage site in specimen F4 and the equivalent location on specimen F3 are shown in figure 20a while gages near the pretest damage site in specimen F4 and the comparable locations in specimen F3 are shown in figure 20b. These results indicate that the damage has little impact on strains for loads less than 41,000 lb, which is the maximum load the specimens were subjected to during the fatigue cycling. However for loading greater than this level, the damage had significant influence on strain behavior in the region of damage, causing loss of load-carrying ability at the damaged skin at a load of approximately 50,000 lb rather than the 83,000 lb found in the undamaged specimen.

Full-field results for axial strains at approximately the maximum applied load are shown in figures 21 and 22 for rod and frame specimens, respectively. The buckle pattern of three half waves in each direction is consistent with the strain distribution shown for the rod specimens. Maximum strain is approximately 0.006 in./in. in magnitude in rod specimen R3. Peak strains are located above the axial centerline where the maximum strain magnitude for specimen R3 is approximately 0.01 in./in. in tension in and approximately -0.01 in./in. in compression at the same location in specimen R4. This difference in direction is representative of the center buckle in one specimen moving toward the camera and in the other specimen moving away from the camera.

In frame specimen F3 the peak axial strains in the OML are located near the specimen corner. In frame specimen F4 peaks in axial strain also occur at the damage site. Since the VIC system only monitors the OML, initiation of failure on the IML could not be captured in this manner.

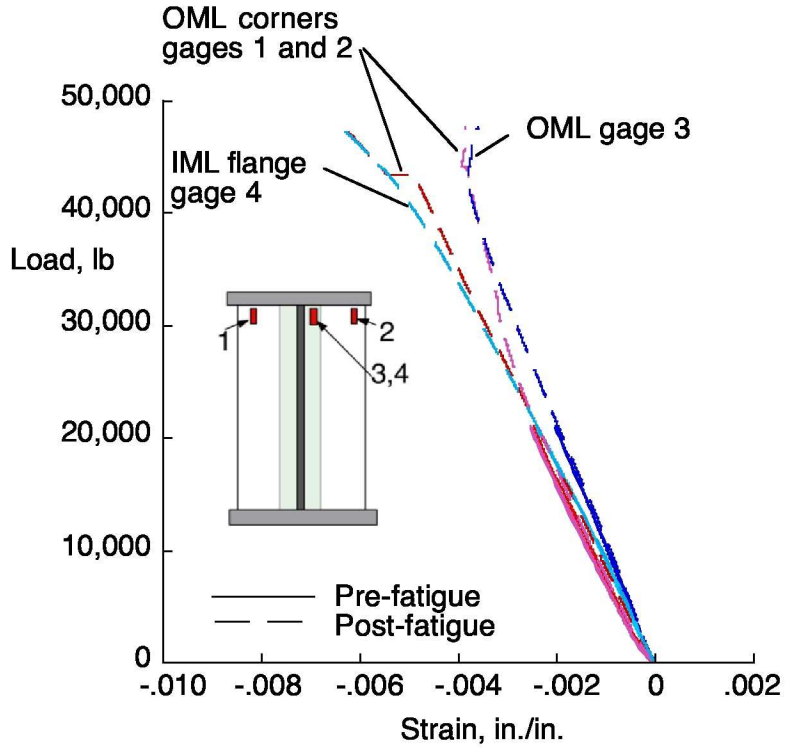


a) Far field gages specimen R3

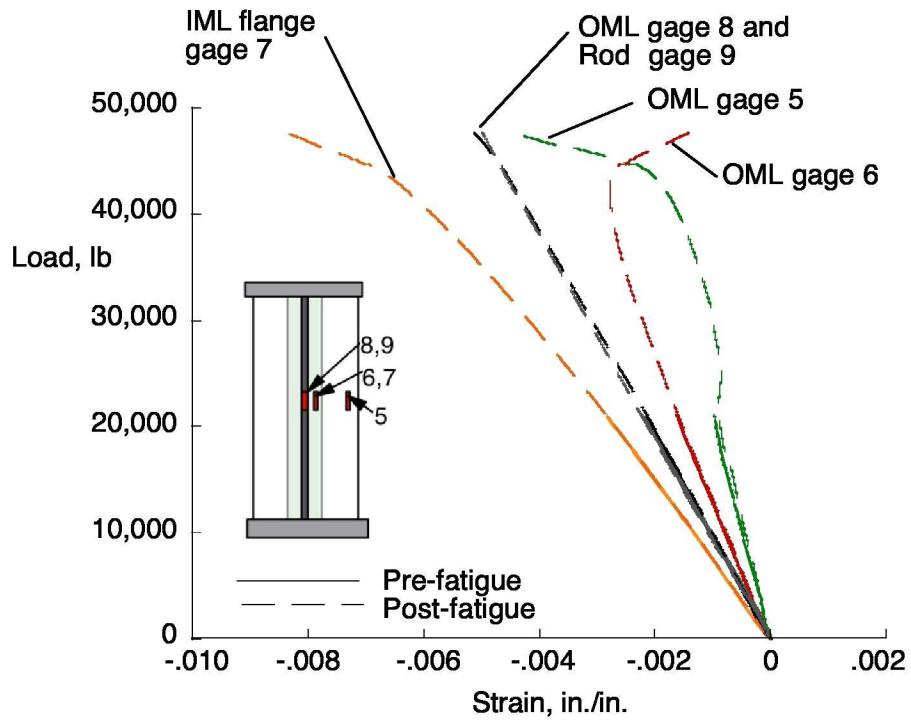


b) Centerline gages specimen R3

Figure 17. Pre-fatigue and post-fatigue strains for rod specimens.

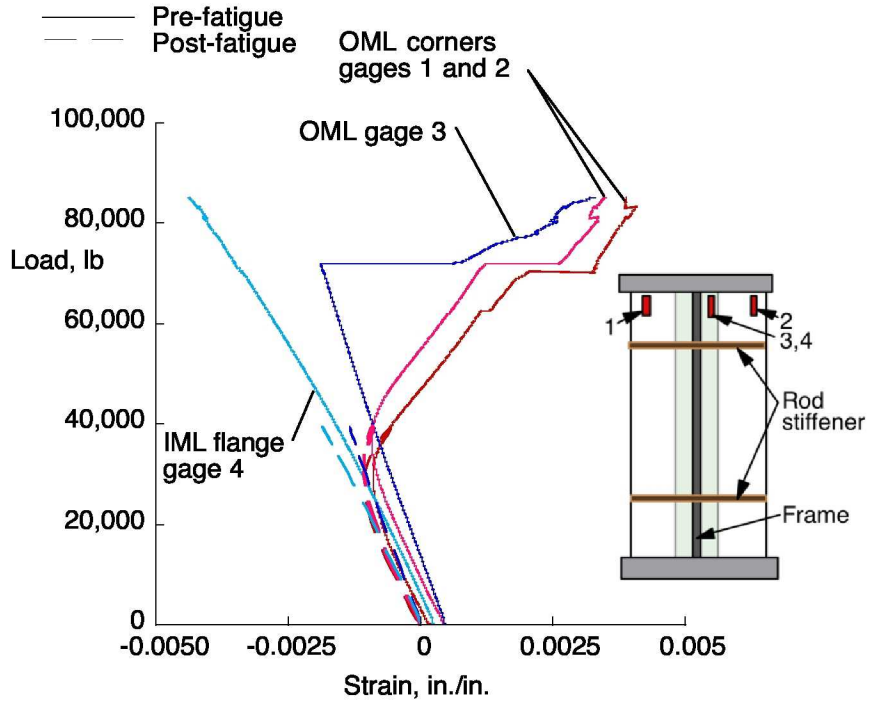


c) Far field gages specimen R4

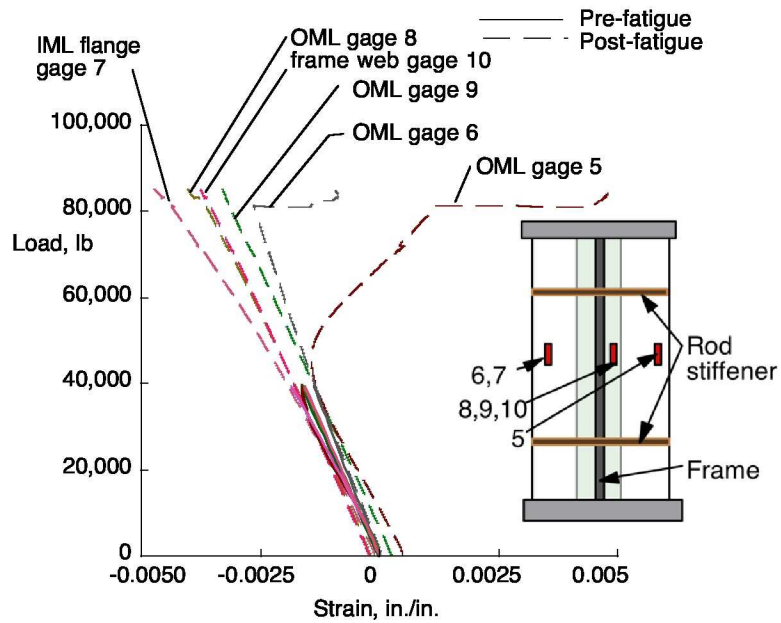


d) Centerline gages specimen R4

Figure 17. Pre-fatigue and post-fatigue strains for rod specimens-continued.

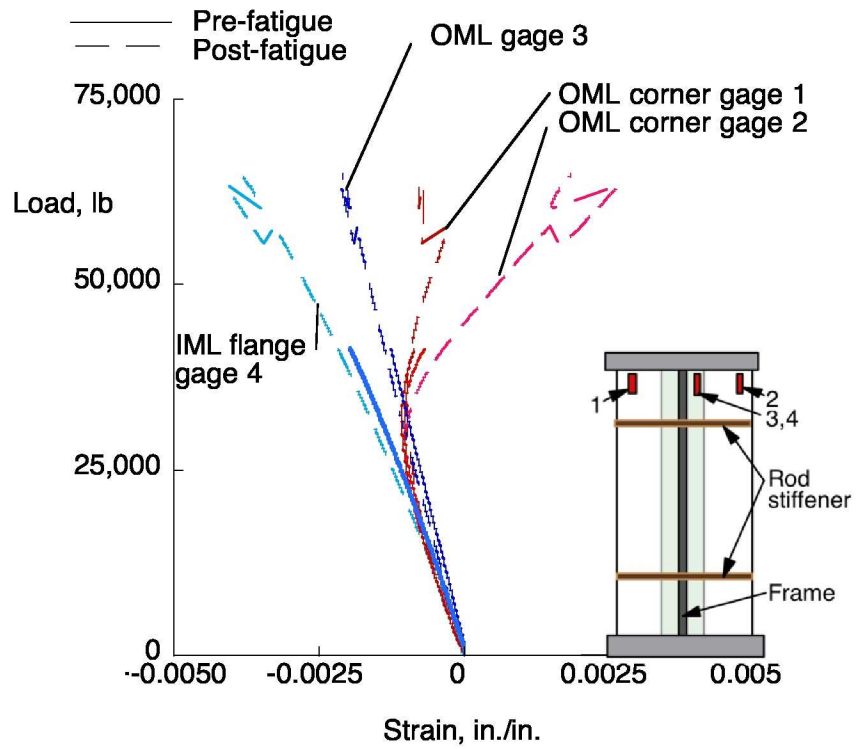


a) Far field gages specimen F3

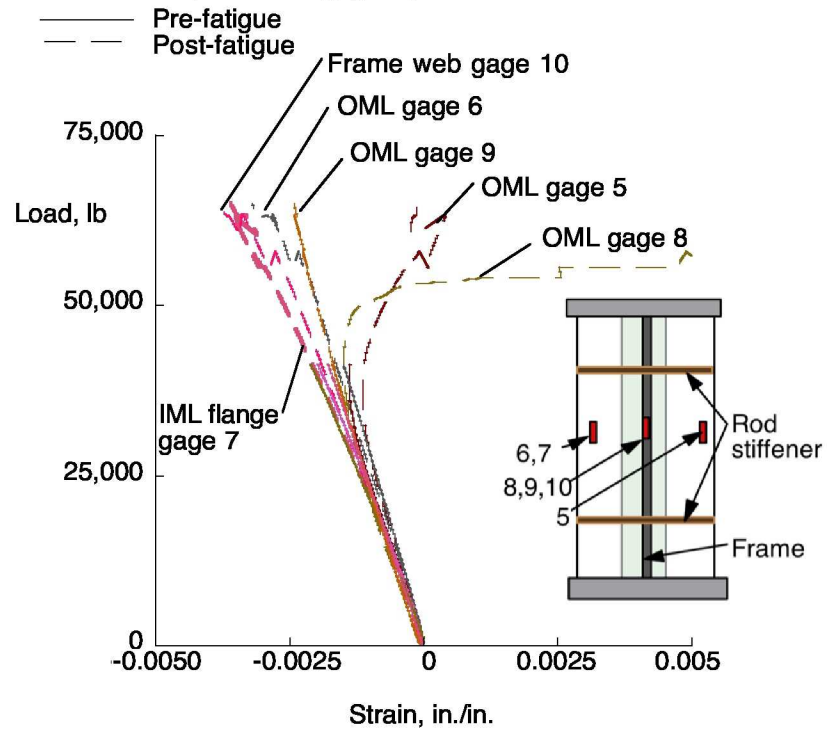


b) Centerline gages specimen F3

Figure 18. Pre-fatigue and Post-fatigue strains for frame specimens.



c) Far field gages specimen F4



d) Centerline gages specimen F4

Figure 18. Pre-fatigue and Post-fatigue strains for frame specimens-continued.

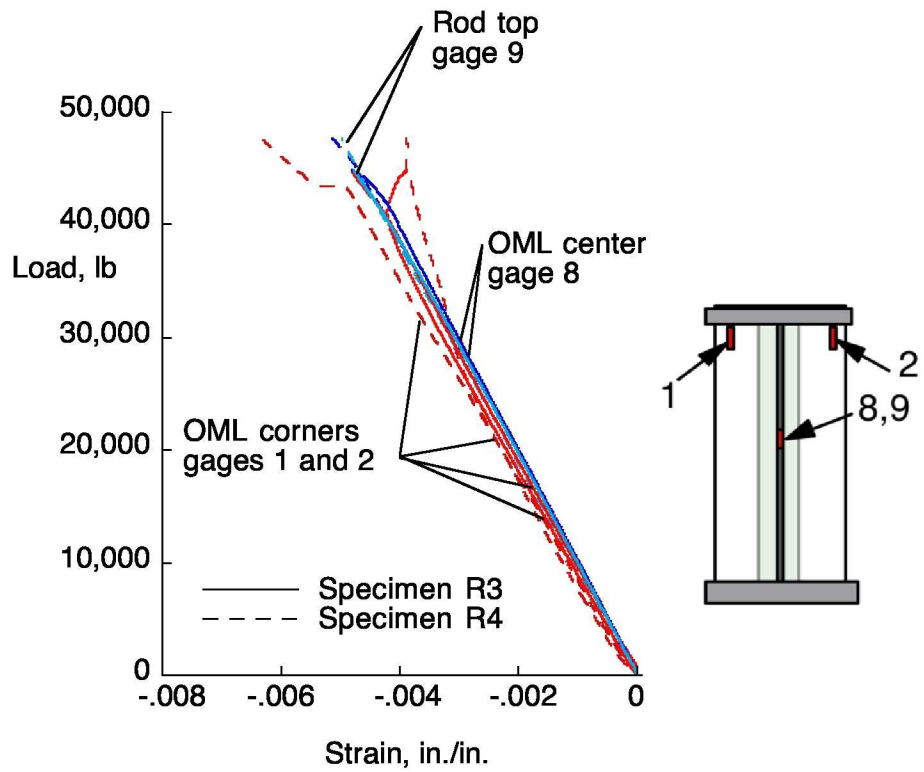
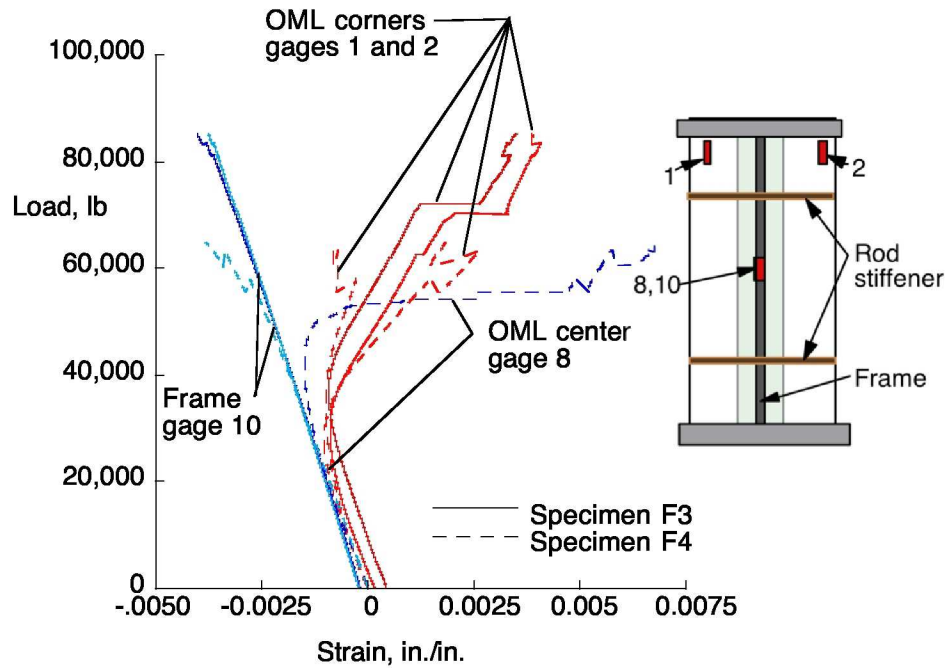


Figure 19. Post-fatigue strains for rod specimens.



a) Away from damage site

Figure 20. Final test strains for frame specimens.

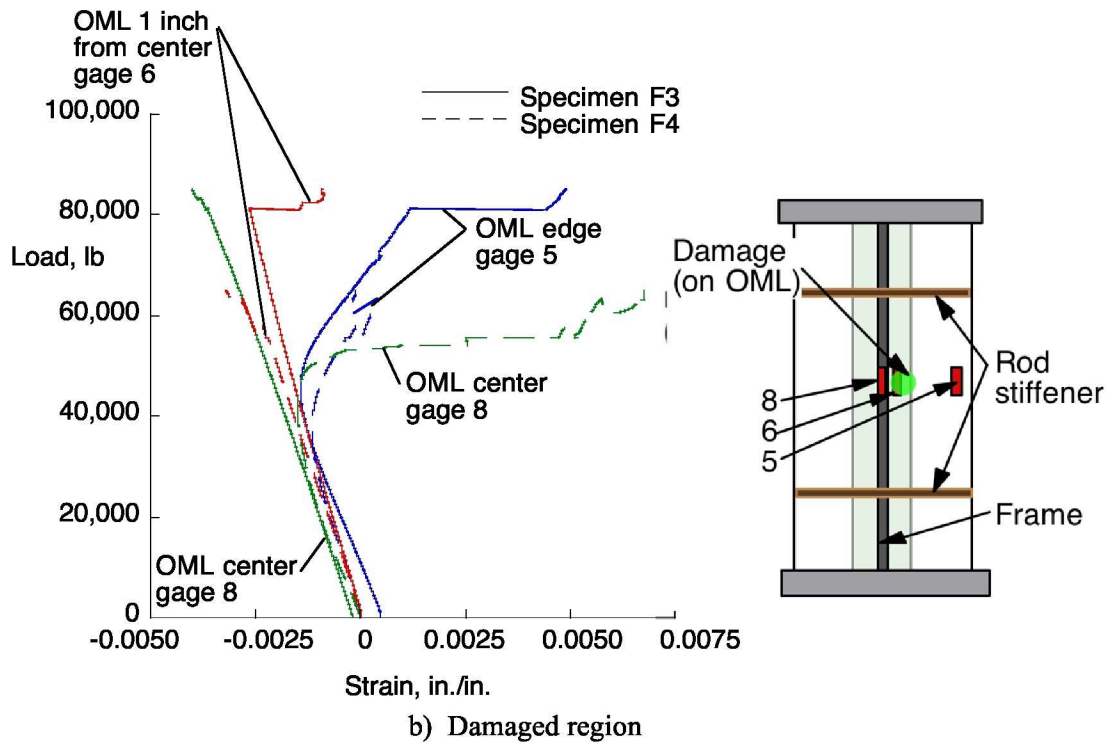


Figure 20. Final test strains for frame specimens-continued.

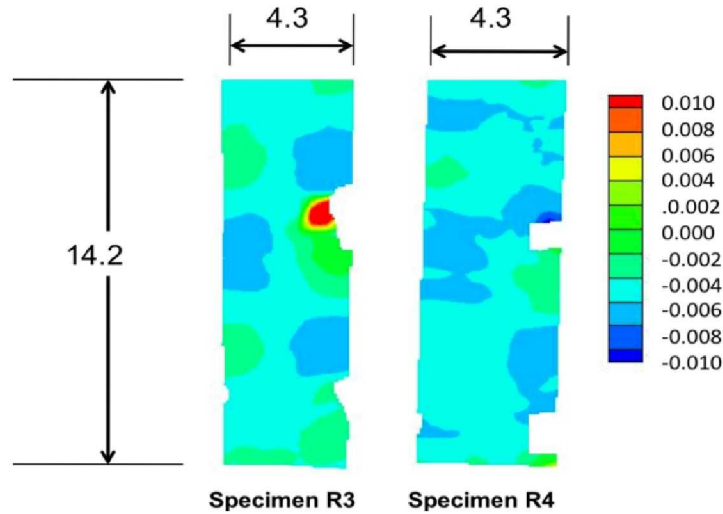


Figure 21. Full field axial strains for rod specimens. Distance shown is in inches. Scale is in in./in.

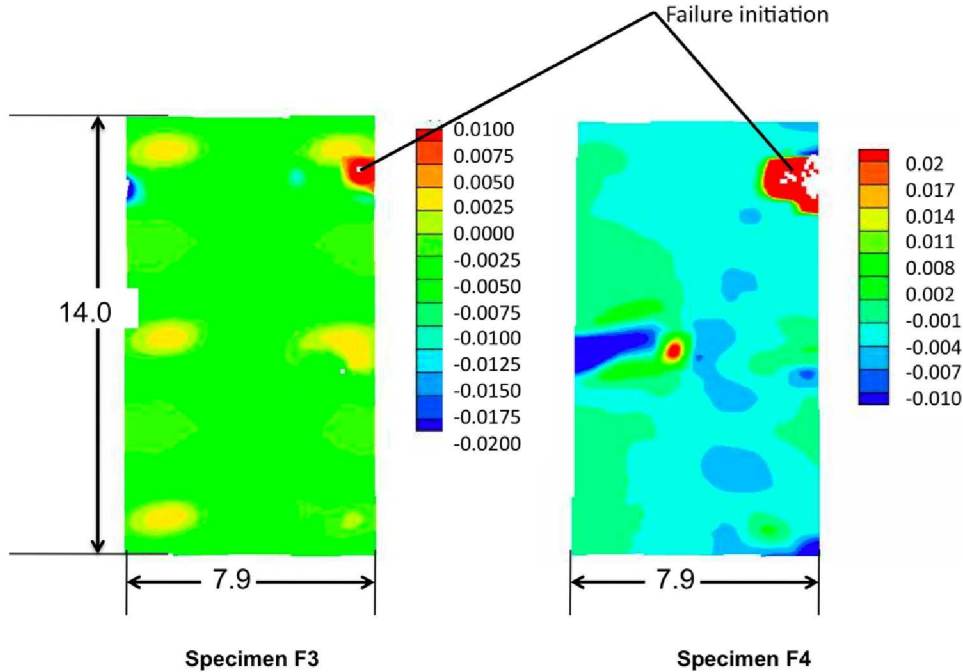


Figure 22. Full field axial strains at failure for frame specimens. Distance shown is in inches. Scale is in in./in.

### Failure

The failure loads the four fatigued specimens as well as nominally identical specimens previously tested under the Boeing contract are shown in table 3 and figure 23. Photographs of failed fatigued rod specimens are shown in figure 24 and failed frame specimens are shown in figure 25.

Rod-stiffened specimens failed midlength across the full width of the specimen. Minimal delamination can be seen between the flange and skin. Overwrap damage can be seen around the rod. Specimens R3 and R4 failed in the same manner. Frame specimen F4 was damaged prior to fatigue cycling but still withstood the cycling with no indication of damage progression and failed at a load equal to 78 percent of the failure load of specimen F3. Failure at the specimen corners and at the top of the location where the rod overwrap intersects the frame is evident in both specimens F3 and F4.

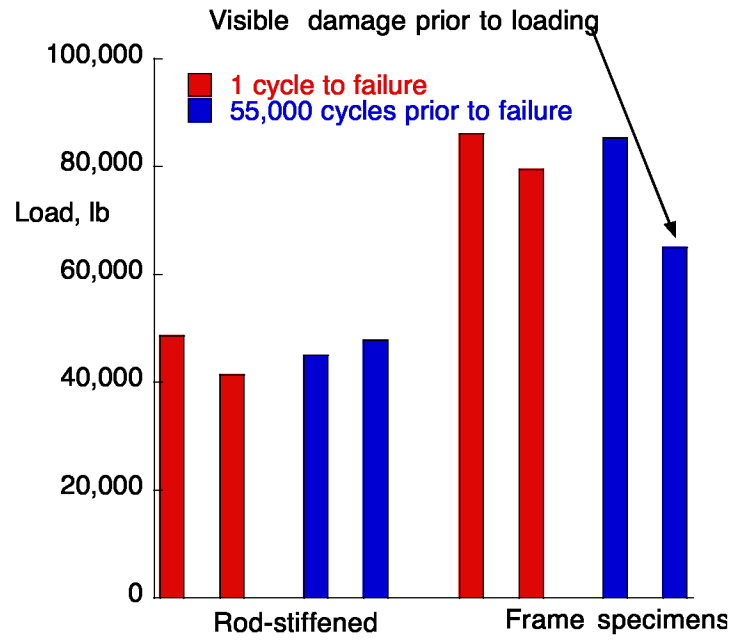


Figure 23. Failure loads.

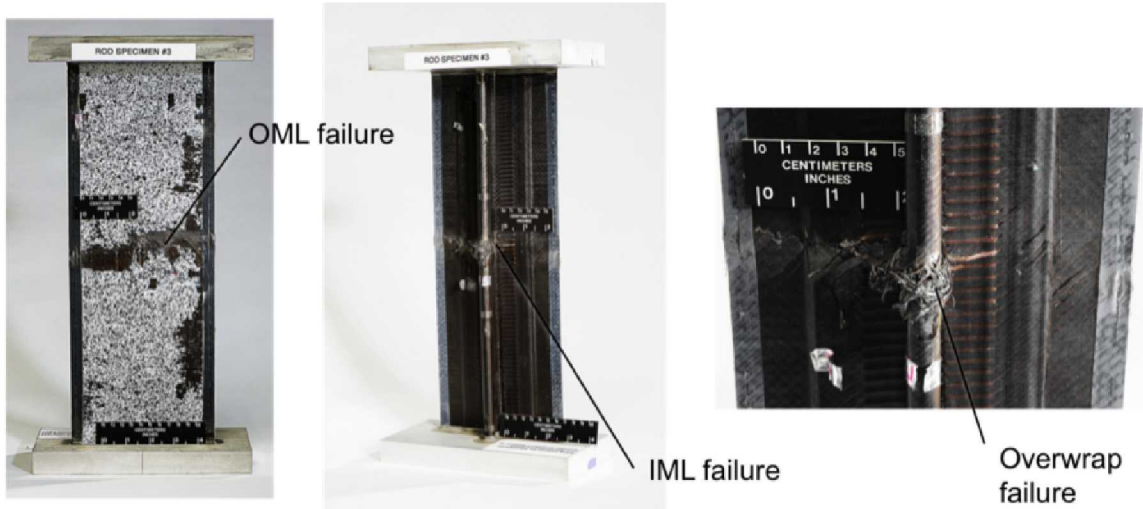
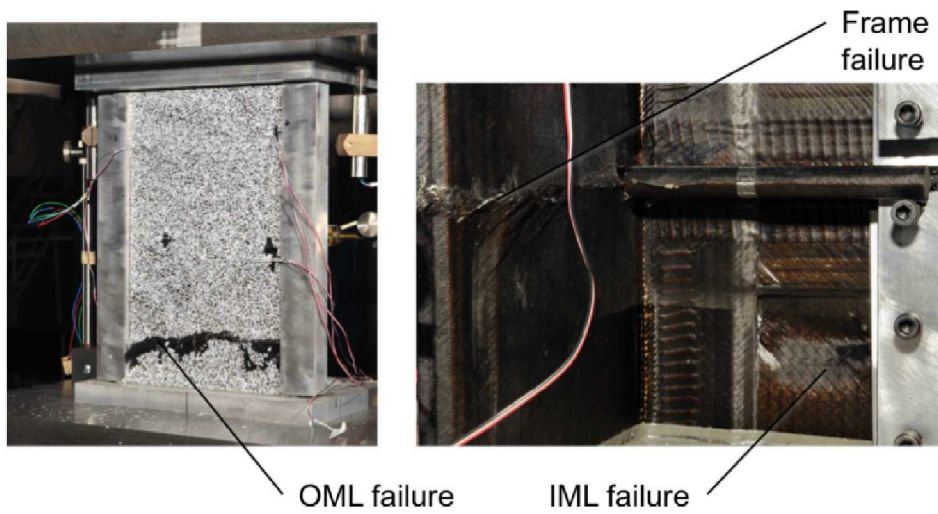
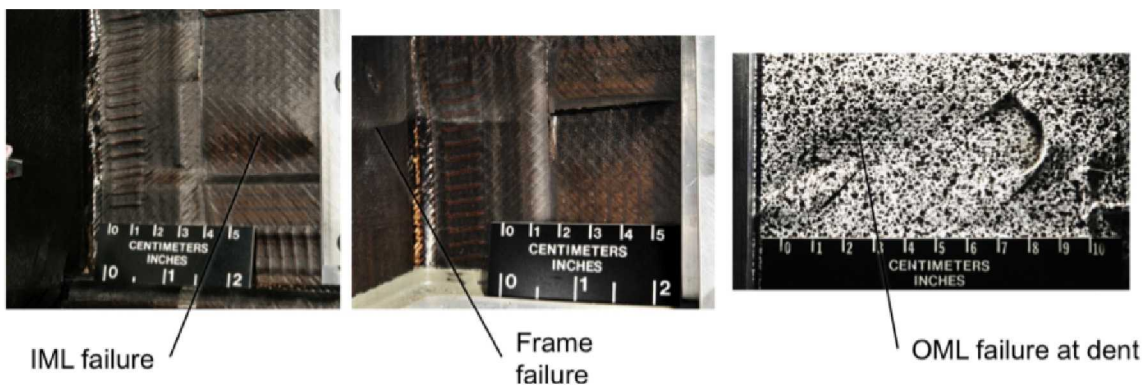


Figure 24. Rod specimen failure.



a) Specimen F3



b) Specimen F4

Figure 25. Frame specimen failure.

## Comparison to past results

Four specimens that were nominally identical to the specimens described herein were loaded in a single test to failure (ref 1). These specimens were cut from the same large panel as the fatigue specimens described herein and tested under the Boeing contract. The failure loads for the NASA-tested and Boeing-tested specimens are shown in table 3 and figure 23 for all eight specimens. Both fatigued rod specimens failed at loads greater than one unfatigued specimen but less than the other unfatigued specimen. Similarly, frame specimen F3 failed at a load greater than one unfatigued specimen but less than the other unfatigued specimen. The fatigued specimens failed in the same manner as the unfatigued specimens. There is no evidence the fatigue cycling had any effect on the failure loads of rod stiffened or frame specimens. Photographs presented in reference 1 show the same failures as seen in specimens R3, R4 and F3. No single-stiffener specimens discussed in reference 1 were damaged prior to loading so no direct comparison to specimen F4 can be made.

## Concluding Remarks

Based on experimental evaluation of nominally identical single-stiffener compression-loaded specimens subjected one or 55,000 cycles of loading, fatigue cycling has no influence on failure load or mode. Visible damage to the skin of a specimen where the frame was loaded in compression reduced the failure load to 78 % of the failure load of the undamaged specimen.

## References

1. Velicki, A., "Damage Arresting Composites for Shaped Vehicles," NASA CR-2009-215932 Sep., 2009.
2. Velicki, A., "Advanced Structural Concept Development Using Stitched Composites." Presented at the 49th AIAA/ASME/ASCE/AHS/ASC Structures, Structural Dynamics and Materials Conference, Chicago Ill, April, 2008.
3. Jegley, D. C, Velicki, A., and Hansen, D. A., "Structural Efficiency Of Stitched Rod-stiffened Composite Panels With Stiffener Crippling." Presented at the 49th AIAA/ASME/ASCE/AHS/ASC Structures, Structural Dynamics and Materials Conference, Chicago Ill, April, 2008.
4. Air Vehicle Technology Integration program (AVTIP), Delivery Order 0059: Multi-role Bomber Structural Analysis, AFRL-VVA-WP-TR-2006-3067, Krishna Hoffman, May 2006, Final Report for 14 December 2004-08 May 2006, AFRL-VA-WP-TR-2006-3067

Table 1. Fatigue Spectrum for a single block\*

	Load (lb) Rod-stiffened	Load (lb) Frame-stiffened
Cycle 1	20,500	41,000
Cycle 2-14	19,500	39,000
Cycle 15-5000	18,500	37,000

\*5000-cycle blocks repeated 11 times for each specimen

Table 2 Load rate and data recorded through fatigue loading

	Load Rate	Data Recorded
<b>Specimen R4</b>		
Block 1-11 Cycle 1-14	4000 lb/min	Cycle 1 each block
Block 1-11 Cycle 15-5000	Approx. 20,000 lb/min	none
<b>Specimen R3</b>		
Block 1-11 Cycle 1	5000 lb/min	Cycle 1 for blocks 1,5,9
Block 1-11 Cycle 2-5000	Approx 20,000 lb/min	none
<b>Specimen F3</b>		
Block 1-11 Cycle 1-14	10,000 lb/min	Cycle 1 blocks 1, 2, 6
Block 1-11 Cycle 15-5000	Approx. 40,000 lb/min	none
<b>Specimen F4</b>		
Block 1-11 Cycle 1	10,000 lb/min	Cycle 1 for blocks 1, 6
Block 1-11 Cycle 2-5000	Approx 40,000 lb/min	none

Table 3 Specimen failure loads\*

Specimen	Test facility	Test type	Failure load (lb)
Rod 1	Boeing	static	48,500
Rod 2	Boeing	static	41,400
R3	NASA	Fatigue/static	45,000
R4	NASA	Fatigue/static	47,654
Frame 1	Boeing	static	86,000
Frame 2	Boeing	static	79,500
F3	NASA	Fatigue/static	85,152
F4	NASA	Fatigue/static (damaged)	64,999

\*Data for specimens at the Boeing test facility are presented in reference 1.

REPORT DOCUMENTATION PAGE			Form Approved OMB No. 0704-0188		
<p>The public reporting burden for this collection of information is estimated to average 1 hour per response, including the time for reviewing instructions, searching existing data sources, gathering and maintaining the data needed, and completing and reviewing the collection of information. Send comments regarding this burden estimate or any other aspect of this collection of information, including suggestions for reducing this burden, to Department of Defense, Washington Headquarters Services, Directorate for Information Operations and Reports (0704-0188), 1215 Jefferson Davis Highway, Suite 1204, Arlington, VA 22202-4302. Respondents should be aware that notwithstanding any other provision of law, no person shall be subject to any penalty for failing to comply with a collection of information if it does not display a currently valid OMB control number.  <b>PLEASE DO NOT RETURN YOUR FORM TO THE ABOVE ADDRESS.</b></p>					
1. REPORT DATE (DD-MM-YYYY) 01-12-2009		2. REPORT TYPE Technical Memorandum		3. DATES COVERED (From - To)	
4. TITLE AND SUBTITLE Experimental Behavior of Fatigued Single Stiffener PRSEUS Specimens			5a. CONTRACT NUMBER		
			5b. GRANT NUMBER		
			5c. PROGRAM ELEMENT NUMBER		
6. AUTHOR(S) Jegley, Dawn C.			5d. PROJECT NUMBER		
			5e. TASK NUMBER		
			5f. WORK UNIT NUMBER 699959.02.08.07.02.02		
7. PERFORMING ORGANIZATION NAME(S) AND ADDRESS(ES) NASA Langley Research Center Hampton, VA 23681-2199			8. PERFORMING ORGANIZATION REPORT NUMBER  L-19782		
9. SPONSORING/MONITORING AGENCY NAME(S) AND ADDRESS(ES) National Aeronautics and Space Administration Washington, DC 20546-0001			10. SPONSOR/MONITOR'S ACRONYM(S)  NASA		
			11. SPONSOR/MONITOR'S REPORT NUMBER(S) NASA/TM-2009-215955		
12. DISTRIBUTION/AVAILABILITY STATEMENT Unclassified - Unlimited Subject Category 39 Availability: NASA CASI (443) 757-5802					
13. SUPPLEMENTARY NOTES					
14. ABSTRACT NASA, the Air Force Research Laboratory and The Boeing Company have worked to develop new low-cost, light-weight composite structures for aircraft. A Pultruded Rod Stitched Efficient Unitized Structure (PRSEUS) concept has been developed which offers advantages over traditional metallic structure. In this concept a stitched carbon-epoxy material system has been developed with the potential for reducing the weight and cost of transport aircraft structure by eliminating fasteners, thereby reducing part count and labor. By adding unidirectional carbon rods to the top of stiffeners, the panel becomes more structurally efficient. This combination produces a more damage tolerant design. This document describes the results of experimentation on PRSEUS specimens loaded in unidirectional compression in fatigue and to failure.					
15. SUBJECT TERMS Composites; Structurally efficient; Lightweight; Graphite-epoxy; Hybrid wing body; Out-of-autoclave; VARTM; Stitched; Buckling					
16. SECURITY CLASSIFICATION OF:			17. LIMITATION OF ABSTRACT	18. NUMBER OF PAGES	19a. NAME OF RESPONSIBLE PERSON
a. REPORT	b. ABSTRACT	c. THIS PAGE			STI Help Desk (email: help@sti.nasa.gov)
U	U	U	UU	31	19b. TELEPHONE NUMBER (Include area code) (443) 757-5802